Rotational invariance and order-parameter stiffness in frustrated quantum spin systems

L. O. Manuel, A. E. Trumper and H. A. Ceccatto
Instituto de Física Rosario, Consejo Nacional de Investigaciones Científicas y Técnicas and Universidad Nacional de Rosario, Bvd. 27 de Febrero 210 Bis, 2000 Rosario, República Argentina

Abstract

We compute, within the Schwinger-boson scheme, the Gaussian-fluctuation corrections to the order-parameter stiffness of two frustrated quantum spin systems: the triangular-lattice Heisenberg antiferromagnet and the J_1-J_2 model on the square lattice. For the triangular-lattice Heisenberg antiferromagnet we found that the corrections weaken the stiffness, but the ground state of the system remains ordered in the classical 120° spiral pattern. In the case of the J_1-J_2 model, with increasing frustration the stiffness is reduced until it vanishes, leaving a small window $0.53 \lesssim \eta \lesssim 0.64$ where the system has no long-range magnetic order. In addition, we discuss several methodological questions related to the Schwinger-boson approach. In particular, we show that the consideration of finite clusters which require twisted boundary conditions to fit the infinite-lattice magnetic order avoids the use of *ad hoc* factors to correct the Schwinger-boson predictions.

I. INTRODUCTION

Two-dimensional (2D) frustrated quantum spin systems are a fascinating subject that has been studied for more than 20 years now. Since the seminal work by Fazekas and Anderson on the $S=\frac{1}{2}$ triangular-lattice Heisenberg antiferromagnet (TLHA), [1] the existence of non-magnetic ground states in these systems has been strongly debated in the literature. In the last years, this problem was somehow linked to more general questions concerning spin-liquid states and their possible connections to high-T_c superconductivity. In this context, the square-lattice Heisenberg antiferromagnet with positive first- and second-neighbor interactions, the so-called J_1-J_2 model, has been much studied. [2] Unlike the TLHA which is frustrated because of the lattice topology, in the J_1-J_2 model frustration is due to the competing couplings.

Regarding the TLHA, although in general there is a growing conviction that this model displays the characteristic 120° spiral order in its ground state (perhaps with an important reduction of the classical $\frac{1}{2}$ value), [4,5,3] using different methods some authors found a situation very close to a critical one or no magnetic long-range order at all. [6,7] We have previously performed a study of the TLHA —including first- and second-neighbor interactions—

using the rotational invariant Schwinger-boson approach in a mean-field (saddle-point) approximation. [8] In particular, for the ground-state energy this method showed a remarkable agreement with exact numerical results on finite lattices (at the time of this work only results for the 12-site cluster were available). Furthermore, the local magnetization in the thermodynamc limit was predicted to be slightly larger than the (harmonic) spin-wave result. More recently, new finite-size results [5,7] and $1/S$-corrected spin-wave calculations [9,10] became available, which lead us to reconsider this model. In this work we present the one-loop corrections to the saddle-point results obtained in [8], along the lines developed in [11,12]. We have computed the ground-state energy and the spin-stiffness tensor in order to assess the existence or not of magnetic order, and we have compared these results with exact values on finite lattices and spin-wave results.

As for the $J_1\!-\!J_2$ model, in previous publications [11,12] we have considered its behavior on finite clusters that do not frustrate the short-range Néel and collinear orders present in this system. In particular, we computed the stiffness ρ to determine the range of $\eta = J_2/J_1$ where the magnetic order is destroyed by the combined action of quantum fluctuations and frustration. However, it turned out to be that the value of ρ obtained at saddle-point order was nearly a factor 2 smaller than exact results on small clusters. This was confirmed by considering the large-S limit of the Schwinger-boson predictions, which differed from the classical results by exactly this factor. The same happened, now for all values of S, in the 2-site problem, which can be worked out exactly. After these checks, in [11,12] we simply added an *ad hoc* factor 2 to correct the saddle-point result for ρ. Although the need for this kind of factors has been stressed since the first works on Schwinger bosons, [13] their use is highly unsatisfactory.

In the course of the present study on clusters of the triangular lattice, again the large-S Schwinger-boson prediction for ρ did not reproduce the classical result. The situation was here even worse than for the square lattice, since now the rotational invariant Schwinger-boson approach could not produce concrete predictions for the stiffness parallel and perpendicular to the plane where the order parameter spirals. In an attempt to resolve this last problem, we followed the idea in [5,10] and considered clusters with appropiate twisted boundary conditions to fit the 120° spiral order in the xy-plane. In this case, since the boundary conditions break the rotational invariance explicitly, one is able to compute the parallel and perpendicular stiffness separately. Moreover, we found that now the large-S predictions for these quantities have the correct behavior and no *ad hoc* factors are required. This unexpected result prompted us to reinvestigate the $J_1\!-\!J_2$ model on clusters which require the use of antiperiodic boundary conditions to avoid frustrating the Néel and collinear orders. Again in this case the results have the expected large-S behavior, and there is no need for correction factors. These findings point to a complex interplay between rotational invariance and the unphysical enlargement of Fock space in the Schwinger-boson approach. Fortunately, working on appropiate clusters the results for both the TLHA and the $J_1\!-\!J_2$ model behave consistently, as we show below.

II. ORDER-PARAMETER STIFFNESS AND THE SCHWINGER-BOSON APPROACH

Let's consider a general Heisenberg model,

$$H = \frac{1}{2} \sum_{\mathbf{r},\mathbf{r}'} J(\mathbf{r} - \mathbf{r}')\ \vec{S}_{\mathbf{r}} \cdot \vec{S}_{\mathbf{r}'} \tag{1}$$

where $\mathbf{r}, \mathbf{r}'$ indicate sites on a two-dimensional lattice. On finite clusters generated by the translation vectors $\mathbf{T}_\alpha$ ($\alpha = 1, 2$) we impose arbitrary boundary conditions $\vec{S}_{\mathbf{r}+\mathbf{T}_\alpha} = \mathcal{R}_{\widehat{n}}(\Phi_\alpha)\vec{S}_{\mathbf{r}}$, where $\mathcal{R}_{\widehat{n}}(\Phi_\alpha)$ is the matrix that rotates an angle Φ_α around some axis $\widehat{n}$ (notice that we are using boldface (arrows) for vectors in real (spin) space). By performing local rotations $\vec{S}_{\mathbf{r}} \to \mathcal{R}_{\widehat{n}}(\theta_{\mathbf{r}})\vec{S}_{\mathbf{r}}$ of angle $\theta_{\mathbf{r}} = \mathbf{Q} \cdot \mathbf{r}$, the Hamiltonian (1) becomes

$$H = \frac{1}{2} \sum_{\mathbf{r},\mathbf{r}'} J(\mathbf{r} - \mathbf{r}') \left\{ (\vec{S}_{\mathbf{r}} \cdot \widehat{n})(\vec{S}_{\mathbf{r}'} \cdot \widehat{n}) + \cos\theta_{\mathbf{r}\mathbf{r}'} \left[\vec{S}_{\mathbf{r}} \cdot \vec{S}_{\mathbf{r}'} - (\vec{S}_{\mathbf{r}} \cdot \widehat{n})(\vec{S}_{\mathbf{r}'} \cdot \widehat{n}) \right] + \sin\theta_{\mathbf{r}\mathbf{r}'} (\vec{S}_{\mathbf{r}} \times \vec{S}_{\mathbf{r}'}) \cdot \widehat{n} \right\}, \tag{2}$$

where $\theta_{\mathbf{r}\mathbf{r}'} = \mathbf{Q} \cdot (\mathbf{r}' - \mathbf{r})$. In this way, with the choice $\mathbf{Q} \cdot \mathbf{T}_\alpha = \Phi_\alpha$ the boundary conditions become the standard periodic ones $\vec{S}_{\mathbf{r}+\mathbf{T}_\alpha} = \vec{S}_{\mathbf{r}}$.

We define the ($T = 0$) stiffness tensor $\rho_{\widehat{n}}$ by

$$\rho_{\widehat{n}}^{\alpha\beta} = \left. \frac{\partial^2 E_{\rm GS}(\mathbf{Q})}{\partial\theta_\alpha \partial\theta_\beta} \right|_{\mathbf{Q}=0}, \tag{3}$$

where $E_{\rm GS}$ is the ground-state energy *per spin* and $\theta_\alpha = \mathbf{Q} \cdot \mathbf{e}_\alpha$ ($\alpha = 1, 2$) are the twist angles along the basis vectors $\mathbf{e}_\alpha$. Then, by using second-order perturbation theory it is simple to prove that $\rho_{\widehat{n}}^{\alpha\beta} = \mathrm{T}_{\widehat{n}}^{\alpha\beta} + \mathrm{J}_{\widehat{n}}^{\alpha\beta}$, where

$$\mathrm{T}_{\widehat{n}}^{\alpha\beta} = \left\langle -\frac{1}{2} \sum_{\mathbf{r}} J(\mathbf{r}) r^\alpha r^\beta \left[\vec{S}_0 \cdot \vec{S}_{\mathbf{r}} - (\vec{S}_0 \cdot \widehat{n})(\vec{S}_{\mathbf{r}} \cdot \widehat{n}) \right] \right\rangle_{\rm GS}, \tag{4}$$

and

$$\mathrm{J}_{\widehat{n}}^{\alpha\beta} = 2 \left\langle \mathrm{j}_{\widehat{n}}^{\alpha}\, P \left(\frac{1}{H - E_{\rm GS}} \right) P\, \mathrm{j}_{\widehat{n}}^{\beta} \right\rangle_{\rm GS}. \tag{5}$$

Here $\mathrm{j}_{\widehat{n}}^{\alpha} = \frac{1}{2} \sum_{\mathbf{r}} J(\mathbf{r}) r^\alpha (\vec{S}_0 \times \vec{S}_{\mathbf{r}}) \cdot \widehat{n}$, $P = 1 - |\mathrm{GS}\rangle\langle \mathrm{GS}|$, and $\mathbf{r} = \sum_\alpha r^\alpha \mathbf{e}_\alpha$. For further use, it is convenient to consider also the rotational average $\overline{\rho}_{xy}$ of the stiffness tensor for $\widehat{n}$ in the xy-plane. With $\widehat{n} = (\sin\theta\cos\phi, \sin\theta\sin\phi, \cos\theta)$ and $\theta = \frac{\pi}{2}$, using $\int_0^{2\pi} \frac{d\phi}{2\pi} n^i n^j = \frac{\delta^{ij}}{2}$ ($i, j = 1, 2$) one obtains $\overline{\rho}_{xy} = \frac{1}{2}(\rho_{\widehat{x}} + \rho_{\widehat{y}})$. Analogously, using $\int \frac{d\theta d\phi}{4\pi} n^i n^j = \frac{\delta^{ij}}{3}$ ($i, j = 1, 3$), for the corresponding average in all directions in spin space one obtains $\overline{\rho} = \frac{1}{3}(\rho_{\widehat{x}} + \rho_{\widehat{y}} + \rho_{\widehat{z}})$.

In the case of classical spins, the only contribution to the stiffness comes from the T-term (4). For quantum spins, besides the fact that the calculations are much more complicated, there is also a very important conceptual difference with the classical case. This is more clearly explained for the simple square-lattice Heisenberg model, where from the Lieb-Mattis theorem we know that the exact ground state must be an isotropic singlet $S = 0$ (there is numerical evidence [5] that this theorem —in principle valid for bipartite lattice— might be conveniently extended to the triangular and other frustrated lattices). Then, if we approach the infinite-lattice behavior using a technique which respects the rotational invariance —like, for instance, the Lanczos method on small clusters—, we only have access to the

stiffness average $\overline{\rho}$. On the other hand, if we use approximate methods that assume an order-parameter symmetry breaking —like ordinary spin-wave theory, for instance—, then both the parallel $\rho_{\parallel}$ and perpendicular $\rho_{\perp}$ stiffness tensors can be computed. There is yet a third possibility, the use of the Schwinger-boson technique, which keeps the rotational invariance on finite lattices and develops a spontaneous symmetry-breaking (through a Bose condensation of the Schwinger bosons) in the thermodynamic limit. We will consider this last method since, in addition to providing us with a fairly reliable computational tool, there are several interesting methodological questions which can be discussed.

First, we represent spin operators in terms of Schwinger bosons: [13] $\vec{S}_i = \frac{1}{2}\mathbf{a}_i^\dagger.\vec{\sigma}.\mathbf{a}_i$, where $\mathbf{a}_\mathbf{i}^\dagger = (a_{i\uparrow}^\dagger, a_{i\downarrow}^\dagger)$ is a bosonic spinor, $\vec{\sigma}$ is the vector of Pauli matrices, and there is a boson-number restriction $\sum_\sigma a_{i\sigma}^\dagger a_{i\sigma} = 2S$ on each site. Thus, we can write the partition function for the Hamiltonian (2) as a functional integral over boson coherent states, which allows a saddle-point expansion to be performed. Following the calculations in [12], which we do not reproduce here, we obtain the fluctuation-corrected ground-state energy as the sum of the saddle-point and one-loop contributions, $E_{\rm GS}(\mathbf{Q}) = E_0(\mathbf{Q}) + E_1(\mathbf{Q})$. We evaluate $E_{\rm GS}(\mathbf{Q})$ on finite lattices in order to avoid the infrared divergencies associated to Bose condensation, which signals the appearance of magnetic long-range order in the ground state. Numerical differentiation of $E_{\rm GS}(\mathbf{Q})$ according to (3) gives finally the spin stiffness.

In what follows we will use this method to study the order-parameter stiffness of both the TLHA and the $J_1 - J_2$ model.

III. TRIANGULAR-LATTICE HEISENBERG ANTIFERROMAGNET

For the triangular lattice, finite clusters with the spatial symmetries of the infinite lattice correspond to translation vectors $\mathbf{T}_1 = (n+m)\mathbf{e}_1 + m\mathbf{e}_2$, $\mathbf{T}_2 = n\mathbf{e}_1 + (n+m)\mathbf{e}_2$, where $\mathbf{e}_1 = (a, 0)$, $\mathbf{e}_2 = (-\frac{1}{2}a, \frac{\sqrt{3}}{2}a)$ (a is the lattice spacing). [5] The number of sites in these diamond-shaped clusters is given by $N = n^2 + m^2 + nm$. When $2n + m$ and $n - m$ are multiples of 3, which corresponds to clusters with $N = 3p$ (p integer), periodic boundary conditions do not frustrate the 120° spiral order. Otherwise, $N = 3p + 1$ and one has to use twisted boundary conditions with angles $\frac{2}{3}\pi(2n + m)$ and $\frac{2}{3}\pi(n - m)$ along the $\mathbf{T}_1$ and $\mathbf{T}_2$ directions, respectively.

Let's consider first the (by far) easiest case of classical spins. Choosing the proper boundary conditions as explained above, the classical energy is minimized by a configuration $\vec{S}_\mathbf{r} = S(\cos\theta_\mathbf{r}, \sin\theta_\mathbf{r}, 0)$. Here $\theta_\mathbf{r} = \mathbf{Q}^\triangle_{\rm spiral}\cdot\mathbf{r}$, with the magnetic wavevector $\mathbf{Q}^\triangle_{\rm spiral} = (\frac{4\pi}{3a}, 0)$. Since we took the spins to lie on the xy-plane, it is necessary to consider both the parallel stiffness $\rho_\parallel \equiv \rho_{\widehat{z}}$ under a twist around $\widehat{z}$, and the perpendicular stiffness $\rho_\perp \equiv \overline{\rho}_{xy}$ for twists around $\widehat{n}$ versors lying on this plane. As mentioned before, for classical spins the only contributions to $\rho_\parallel$, $\rho_\perp$ and $\overline{\rho}$ come from the T term (4), and one always obtains the tensorial structure $\rho^{\alpha\beta} = \frac{1}{2}(1 + \delta^{\alpha\beta})\rho$ with $\rho_\parallel = JS^2a^2$, $\rho_\perp = \frac{1}{2}\rho_\parallel$ and $\overline{\rho} = \frac{2}{3}\rho_\parallel$. These last two results are consecuences of the identities $\overline{\rho}_{xy} = \frac{1}{2}(\rho_{\widehat{x}} + \rho_{\widehat{y}})$ and $\overline{\rho} = \frac{1}{3}(\rho_{\widehat{x}} + \rho_{\widehat{y}} + \rho_{\widehat{z}})$, plus the fact that $\rho_{\widehat{x}} = \frac{1}{6}\rho_\parallel$ and $\rho_{\widehat{y}} = \frac{5}{6}\rho_\parallel$ for the classical spiral arrangement we choosed.

In order to correct these results by considering the quantum nature of the spins we have followed the procedure discussed in the previous section. On the $N = 3p$ clusters with periodic boundary conditions our approach is rotationally invariant and we only have access

to $\overline{\rho}$. Since now $\rho_{\|}$ and $\rho_{\perp}$ are unrelated, the theory cannot produce concrete predictions for them from $\overline{\rho}$. On the other hand, we found that the large-S Schwinger-boson prediction for this last quantity is exactly 4/3 smaller than the corresponding classical result. As mentioned in the introduction, in an attempt to resolve the former problem we followed the idea in [5,10], and considered the $N = 3p+1$ clusters with the appropiate twisted boundary conditions to fit the 120° spiral order in the xy-plane. In this case, since the boundary conditions break the rotational invariance explicitly, one is able to compute the parallel and perpendicular stiffness separately. Furthermore, we found that now the large-S predictions have the correct behavior and no *ad hoc* factors are required.

In Fig. 1 we present the results for the energy of the $N = 3p$ clusters, together with results from exact diagonalization studies [3,4]. As can be seen, for $N = 12, 36$, after the inclusion of Gaussian fluctuations our theory gives predictions very close to the exact ones. However, for $N = 21, 27$ the agreement is not so good. This can be explained by noticing that for odd number of sites the true ground state has total spin $S = 1/2$, while the approximate Schwinger-boson wave function is always a singlet (rotational symmetries are broken only in the thermodynamic limit by the boson condensate). The difference between even and odd N is also apparent in the exact results, since these do not line up according to the expected (spin-wave) scaling. However, following [3], after substracting the top inertial effects in the exact results for the odd-N clusters, our results and these corrected values are in very good agreement (see Fig. 1). This problem becomes less important for larger clusters. The inset in Fig. 1 shows the thermodynamic-limit extrapolation on large lattices of both the $N = 3p$ and $N = 3p + 1$ types (notice that for the $N = 3p$ clusters the linear trend has a slope rather different than what one would obtain from the consideration of the smallest clusters). As discussed above, the $N = 3p + 1$ clusters require twisted boundary conditions to avoid frustrating the spiral order. The main consecuence of this is the absence of rotational symmetry in the ground state, since the boundary conditions choose a plane of magnetization (the xy-plane in this case). Consequently, the scaling of the energy to the thermodynamc limit has a quite different slope than the corresponding to $N = 3p$ clusters, although, of course, the final value for the ground-state energy *per site* $E_{\rm GS} \simeq -0.5533$ is the same in both cases. This happens, as expected, with the results at saddle-point order and also after the inclusion of Gaussian fluctuations.

The finite-size scaling of the parallel stiffness is shown in Fig. 2. In this figure we plot both the saddle-point and fluctuation-corrected results, which run almost parallel to each other. The first-order spin-wave result of [10] is also given for comparison. Notice that, in spite of the different slope, the extrapolated values do not differ much. As a further comparison, in Fig. 3 we plot the renormalization factor between quantum and classical results for the parallel stiffness on small lattices, as given by different techniques. As can be seen from this figure, the introduction of Gaussian-fluctuation corrections to the saddle-point Schwinger-boson results gives values closer to the exact ones than those of first-order spin-wave theory.

IV. J_1–J_2 MODEL

For the square lattice, finite clusters of $N = \sqrt{n^2+m^2} \times \sqrt{n^2+m^2}$ sites correspond to translation vectors $\mathbf{T}_1 = n\mathbf{e}_1 + m\mathbf{e}_2$, $\mathbf{T}_2 = -m\mathbf{e}_1 + n\mathbf{e}_2$, where $\mathbf{e}_1 = (a, 0)$, $\mathbf{e}_2 = (0, a)$.

If n, m are even, the periodic boundary conditions do not frustrate the short-range Néel ($\mathbf{Q}^{\square}_{\text{Néel}} = (\frac{\pi}{a}, \frac{\pi}{a})$) and collinear ($\mathbf{Q}^{\square}_{\text{coll}} = (\frac{\pi}{a}, 0)$) orders present for $\eta = J_2/J_1 \ll 1$ and $\eta \simeq 1$ respectively. For n and/or m odd one has to impose antiperiodic boundary conditions to fit both magnetic patterns to the cluster shape.

Let's assume that the classical energy is minimized by a spin configuration $\vec{S}_{\mathbf{r}} = S(\cos\theta_{\mathbf{r}}, \sin\theta_{\mathbf{r}}, 0)$. For simplicity we consider first the square lattice with nearest-neighbor interactions only, so that $\theta_{\mathbf{r}} = \mathbf{Q}^{\square}_{\text{Néel}} \cdot \mathbf{r}$. Then, from (4) one obtains the tensorial structure $\rho^{\alpha\beta} = \rho\delta^{\alpha\beta}$, where, like for the triangular lattice, $\rho_{\parallel} = JS^2a^2$, $\rho_{\perp} = \frac{1}{2}\rho_{\parallel}$ and $\overline{\rho} = \frac{2}{3}\rho_{\parallel}$. Notice however that for collinear spin arrangements like the Néel order there is properly no perpendicular stiffness. In fact, the value of $\rho_{\perp}$ is obtained from $\overline{\rho}_{xy} = \frac{1}{2}(\rho_{\widehat{x}} + \rho_{\widehat{y}})$ and $\rho_{\widehat{x}} = 0$, $\rho_{\widehat{y}} = \rho_{\parallel}$ for vectors pointing in the $\pm\widehat{x}$ directions. In the same way, the value of $\overline{\rho}$ is a consequence of the identity $\overline{\rho} = \frac{1}{3}(\rho_{\widehat{x}} + \rho_{\widehat{y}} + \rho_{\widehat{z}})$.

In previous publications [11,12] we have considered finite clusters with periodic boundary conditions. Then, we determined $\overline{\rho}$ and, from this quantity, $\rho_{\parallel} = \frac{3}{2}\overline{\rho}$. However, it turned out to be that the results obtained at saddle-point order for $\rho_{\parallel}$ were nearly a factor 2 smaller (or, like in the triangular lattice, the results for $\overline{\rho}$ nearly 4/3 smaller) than exact results on small clusters. As pointed out in the introduction, this was confirmed by considering the large-S limit of the Schwinger-boson predictions, which differed from the classical results by exactly these factors. Moreover, the same happened for all values of S in the 2-site problem, which can be worked out exactly. After these checks, in [11,12] we simply added an *ad hoc* factor 2 to correct the saddle-point result for $\rho_{\parallel}$. The need for this kind of factors is related to a subtle interplay between rotational invariance and the relaxation of the local boson-number restriction, a claim that can be substantiated by the following argument. At saddle-point order the energy $E_{\text{GS}}(\mathbf{Q}) = \frac{1}{2}\sum_{\mathbf{r}} J(\mathbf{r})[B^2_{\mathbf{r}}(\mathbf{Q}) - A^2_{\mathbf{r}}(\mathbf{Q})]$, where $B_{\mathbf{r}}(\mathbf{Q})$ and $A_{\mathbf{r}}(\mathbf{Q})$ are the order parameters for the spin-spin interaction in the ferromagnetic and antiferromagnetic channels respectively. At the same order in the calculations, the exact (local) constraints would force the identity $B^2_{\mathbf{r}}(\mathbf{Q}) + A^2_{\mathbf{r}}(\mathbf{Q}) \equiv S^2$, which shows that both order parameters should contribute in the same way to the stiffness (3). Moreover, the same identity indicates that $(\frac{\partial A_{\mathbf{r}}}{\partial \mathbf{Q}})^2 + (\frac{\partial B_{\mathbf{r}}}{\partial \mathbf{Q}})^2 \equiv -(A_{\mathbf{r}}\frac{\partial^2 A_{\mathbf{r}}}{\partial \mathbf{Q}\partial \mathbf{Q}} + B_{\mathbf{r}}\frac{\partial^2 B_{\mathbf{r}}}{\partial \mathbf{Q}\partial \mathbf{Q}})$. However, when the constraints are imposed on average the order parameters behave independently, the identity is violated, and this last relationship is not fulfilled (the l.h.s. vanishes). On the other hand, on clusters with antiperiodic boundary conditions, which break the rotational invariance, this relationship between derivatives does come right and leads to the correct value for the stiffness, as shown below.

In Fig. 4 we plot the spin stiffness of the J_1–J_2 model on large clusters with antiperiodic boundary conditions (we considered $\eta = 0$ and 0.5 as examples). As expected, the points line up according to the scaling behavior $\rho_{\parallel} \sim N^{-1/2}$. This extrapolation to the thermodynamic limit for several values of η produces the result shown in Fig. 5. There we see a small window ($\sim [0.53, 0.60]$) where the stiffness vanishes and there is no magnetic order (compare with the bottom panel in Fig. 3 of [12]). The inset shows the scaling behavior of the point $\eta^c_{\text{Néel}}$ where the Néel-order stiffness vanishes. Actually, the region without long-range order extends at least up to $\eta \simeq 0.64$, since, as shown in [12], for $0.60 \lesssim \eta \lesssim 0.64$ the short-range antiferromagnetic order has lower energy than the long-range collinear one.

Let's consider also the scaling of the ground-state energy with N, $E^N_{\text{GS}}(\mathbf{Q}^{\square}_{\text{Néel}}) \simeq E_{\text{GS}}(\mathbf{Q}^{\square}_{\text{Néel}}) - a/N^{3/2}$, along the series of clusters with periodic and antiperiodic bound-

ary conditions. The inset in Fig. 6 shows that both series extrapolate to the same value ($E_{\mathrm{GS}}(\mathbf{Q}^{\square}_{\text{Néel}}) \simeq -0.5015$ for $\eta = 0.5$, within numerical errors), although with quite different slopes a. It is of some interest to discuss the behavior of a, which, for periodic boundary conditions, is proportional to the spin-wave velocity (or its anisotropy average) [14]. Working on clusters with periodic boundary conditions, in our previous publication [12] we found an anomalous behavior of a near the point where the collinear order is melted (see Fig. 3 in [12]). In the present work, for clusters with antiperiodic boundary conditions, a has a behavior more in line with *a priori* expectations (see Fig. 6).

V. CONCLUSIONS

We have considered the Gaussian-fluctuation corrections to the spin stiffness of two frustrated quantum spin systems of interest: the TLHA and the $J_1 - J_2$ model. For the TLHA we found that the fluctuation corrections weaken the stiffness, but the ground state of the system remains ordered in the classical 120° spiral state. In the case of the $J_1 - J_2$ model, with increasing frustration the stiffness is reduced until it vanishes, leaving a small window $0.53 \lesssim \eta \lesssim 0.64$ where the system has no long-range magnetic order.

In the course of this investigation we discussed several methodological questions related to the Schwinger-boson approach we used. In particular, we showed that the consideration of clusters which require twisted boundary conditions to fit the magnetic orders avoids the use of *ad hoc* factors to correct the Schwinger-boson predictions. This fact points to a subtle interplay between rotational invariance and the relaxation of local constraints in this approach.

Finally, it is interesting to notice that for both the square and triangular lattices with only nearest-neighbor interactions the fluctuation-corrected spin stiffness scale almost parallel to the saddle-point results (see Figs. 2 and 4), although the corrections have different sign. On the contrary, for large frustration in the square lattice the one-loop result have a very different slope than the zero-order one, which ultimately leads to disordering the system. This difference reflects the distinct nature of the order-parameter fluctuations in this highly frustrated system.

REFERENCES

[1] P. Fazekas and P. W. Anderson, Phil. Mag. **30**, 423 (1974).

[2] A. V. Dotsenko and O. P. Sushkov, Phys. Rev. B **50**, 13821 (1994) and references therein.

[3] B. Bernu, C. Lhuillier, and L. Pierre, Phys. Rev. Lett.**69**, 2590 (1992);

[4] D. A. Huse and V. Elser. Phys. Rev. Lett. **60**, 2531 (1988); R. Deutscher and H. U. Everts, Z. Phys. B **93**, 77 (1993). Phys. Rev. Lett. **60**, 2531 (1988).

[5] B. Bernu, P. Lecheminant, C. Lhuillier, and L. Pierre, Phys. Rev. B **50**, 10048 (1994).

[6] H. Nishimori and H. Nakanishi, J. Phys. Soc. Jpn **57**, 626 (1988); **58**, 2607 (1989); **58** 3433 (1989); N. Eltsner, R. R. P. Singh, and A. P. Young, Phys. Rev. Lett. **71** , 1629 (1993); K. Yang, L. K. Warman , and S. M. Girvin, Phys. Rev. Lett. **70**, 2641 (1993).

[7] P. W. Leung and K. Runge, Phys. Rev. B **47**, 5861 (1993).

[8] C. J. Gazza and H. A. Ceccatto, J. Condens. Matt. **5**, L135 (1993).

[9] A. Chubukov, S. Sachdev, and T. Senthil, J. Phys.: Condens. Matter **6**, 8891 (1994).

[10] P. Lecheminant, B. Bernu, C. Lhuillier, and L. Pierre, Phys. Rev. B **52**, 9162 (1995).

[11] A. E. Feiguin, C. J. Gazza, A. E. Trumper, and H. A. Ceccatto, Phys. Rev. B **52**, 15053 (1995).

[12] A. E. Trumper, L. O. Manuel, C. J. Gazza, and H. A. Ceccatto, Phys. Rev. Lett. **78**, 2216 (1997).

[13] A. Auerbach and D. Arovas, Phys. Rev. Lett. **61**, 617 (1988); Phys. Rev. B **38**, 316 (1988).

[14] H. J. Schulz, T. A. L. Ziman, and D. Poiblanc, J. Physique I, **6**, 675 (1996).

FIGURES

FIG. 1: Ground-state energy *per site* $E_{\rm GS}^{N}$ for the TLHA as a function of the number of sites N in the cluster. Open and full circles give the saddle-point and fluctuation-corrected results, respectively; pluses are exact numerical results from [7] and crosses are the rotational corrected values from [3]. The line indicates the extrapolation to the thermodynamic limit. Inset: Extrapolation to the infinite lattice along the series of clusters with periodic (full circles) and twisted (full squares) boundary conditions.

FIG. 2: Parallel stiffness $\rho_{\|}$ for the TLHA as a function of the number of sites N in the cluster. Open and full circles give the saddle-point and fluctuation-corrected results, respectively. The full lines indicate the thermodynamic-limit extrapolations and the dashed line is the first-order spin-wave result of [10].

FIG. 3: The renormalizaton factor $Z_{\|} = \rho_{\|}/\rho_{\|}^{\rm Cl}$ for the TLHA on small clusters. Open and full circles correspond to saddle-point (SP) and fluctuation-corrected (FL) results, respectively. The exact values (EX) and first-order spin-wave (SW) results, indicated by crosses and open squares respectively, are taken from [10].

FIG. 4: Spin stiffness $\rho_{\|}$ for the J_1–J_2 model as a function of the number of sites N in the cluster. Top panel: $\eta = 0$; bottom panel: $\eta = 0.5$. Open and full circles give the saddle-point and fluctuation-corrected results, respectively. The lines indicate the thermodynamic-limit extrapolation.

FIG. 5: Spin stiffness $\rho_{\|}$ for the J_1–J_2 model extrapolated to the thermodynamic limit. Dashed and full lines correspond to saddle-point and fluctuation-corrected results, respectively. Inset: Extrapolation of the critical value $\eta_{\rm c} = J_{2\rm c}/J_1$ where the Néel-order stiffness vanishes.

FIG. 6: Slope a of the scaling $E_{\rm GS}^{N}$ vs. $N^{-3/2}$ on clusters with antiperiodic boundary conditions. The inset shows the scaling of the ground-state energy $E_{\rm GS}^{N}$ on clusters with periodic (full circles) and antiperiodic (full squares) boundary conditions for $\eta = 0.5$.

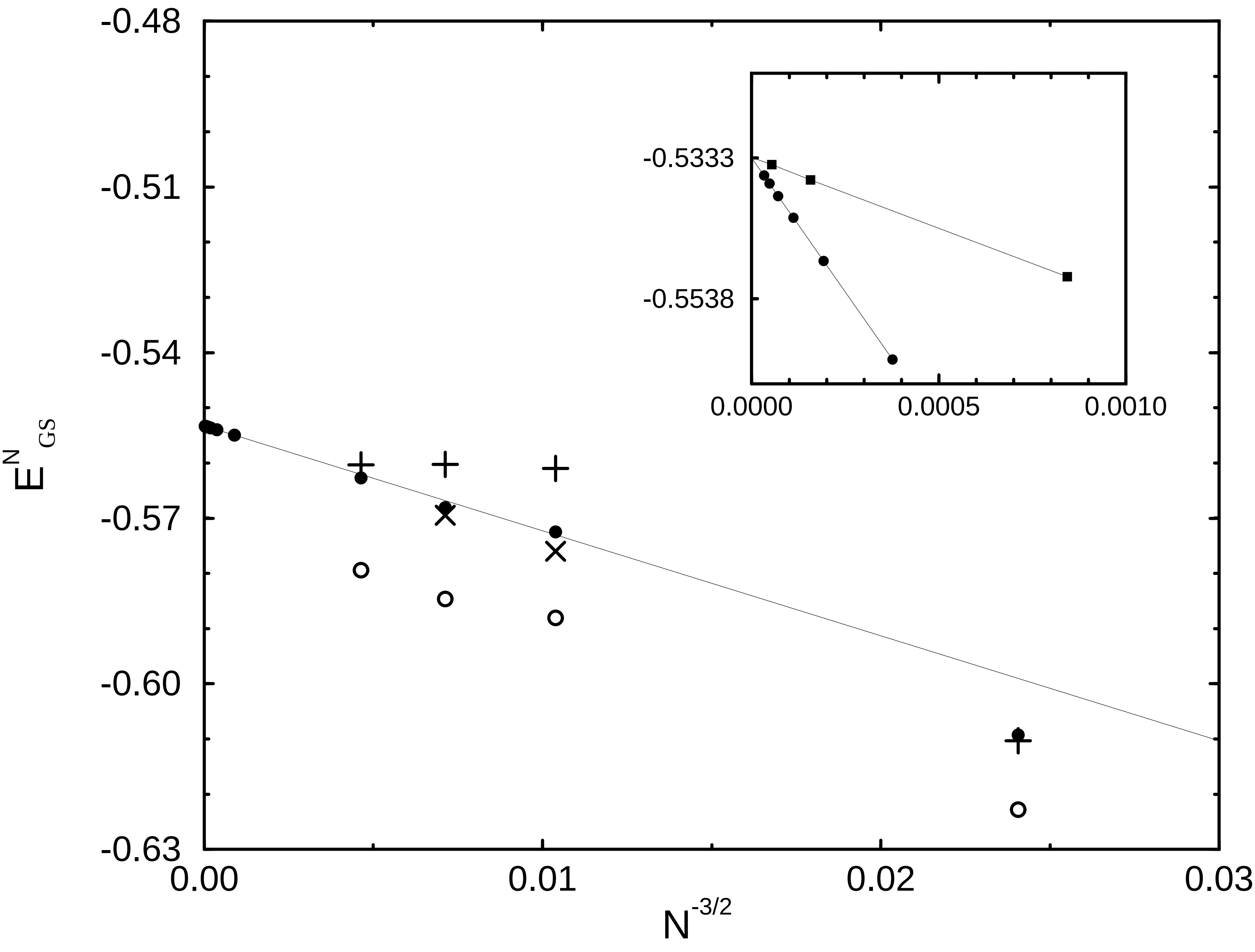

-0.48
-0.51
-0.54
-0.57
-0.60
-0.63
0.00
0.01
0.02
0.03
E^N_{GS}
$N^{-3/2}$
-0.5333
-0.5338
0.0000
0.0005
0.0010

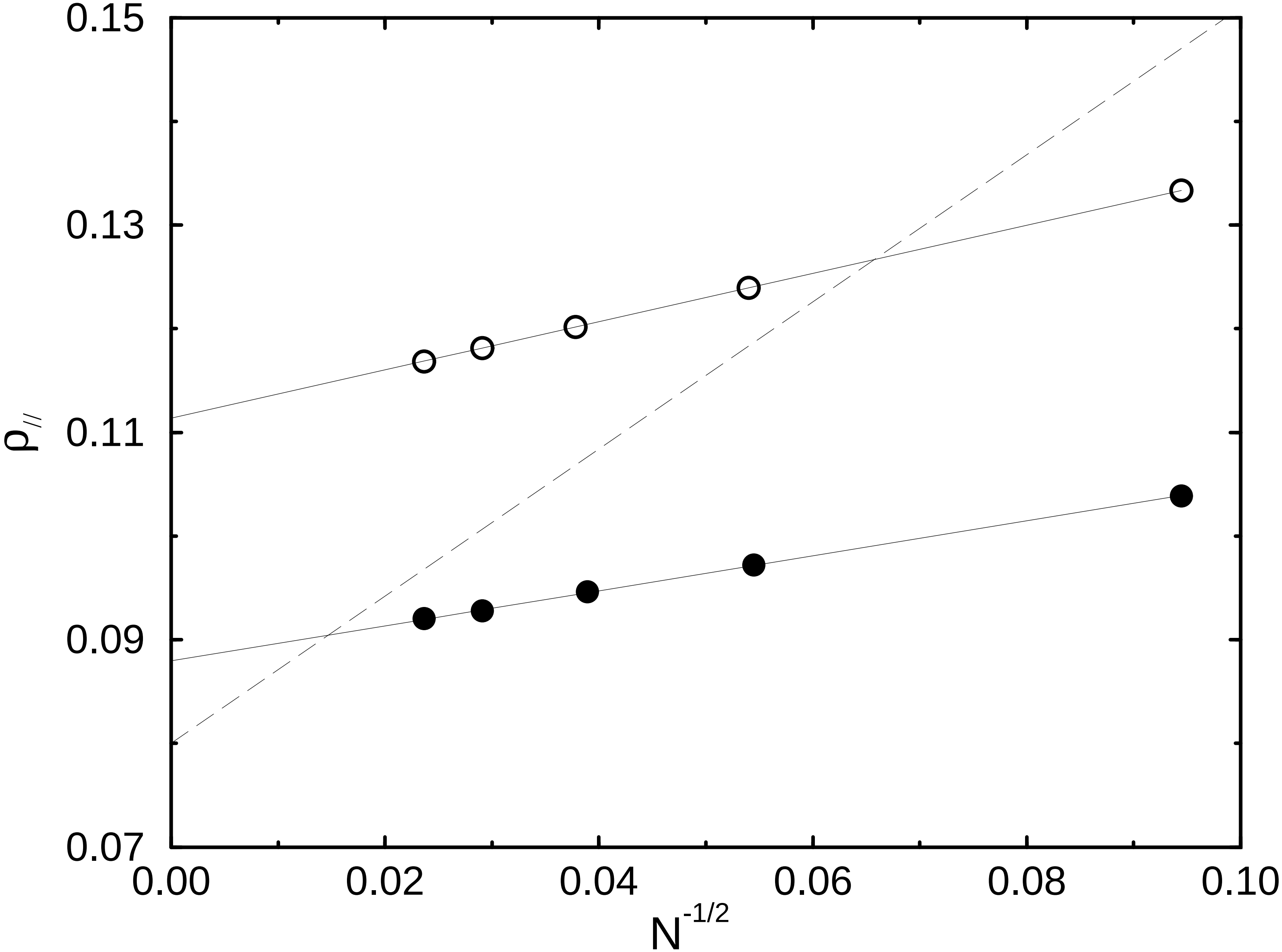

0.15
0.13
0.11
0.09
0.07
ρ//
0.00
0.02
0.04
0.06
0.08
0.10
N-1/2

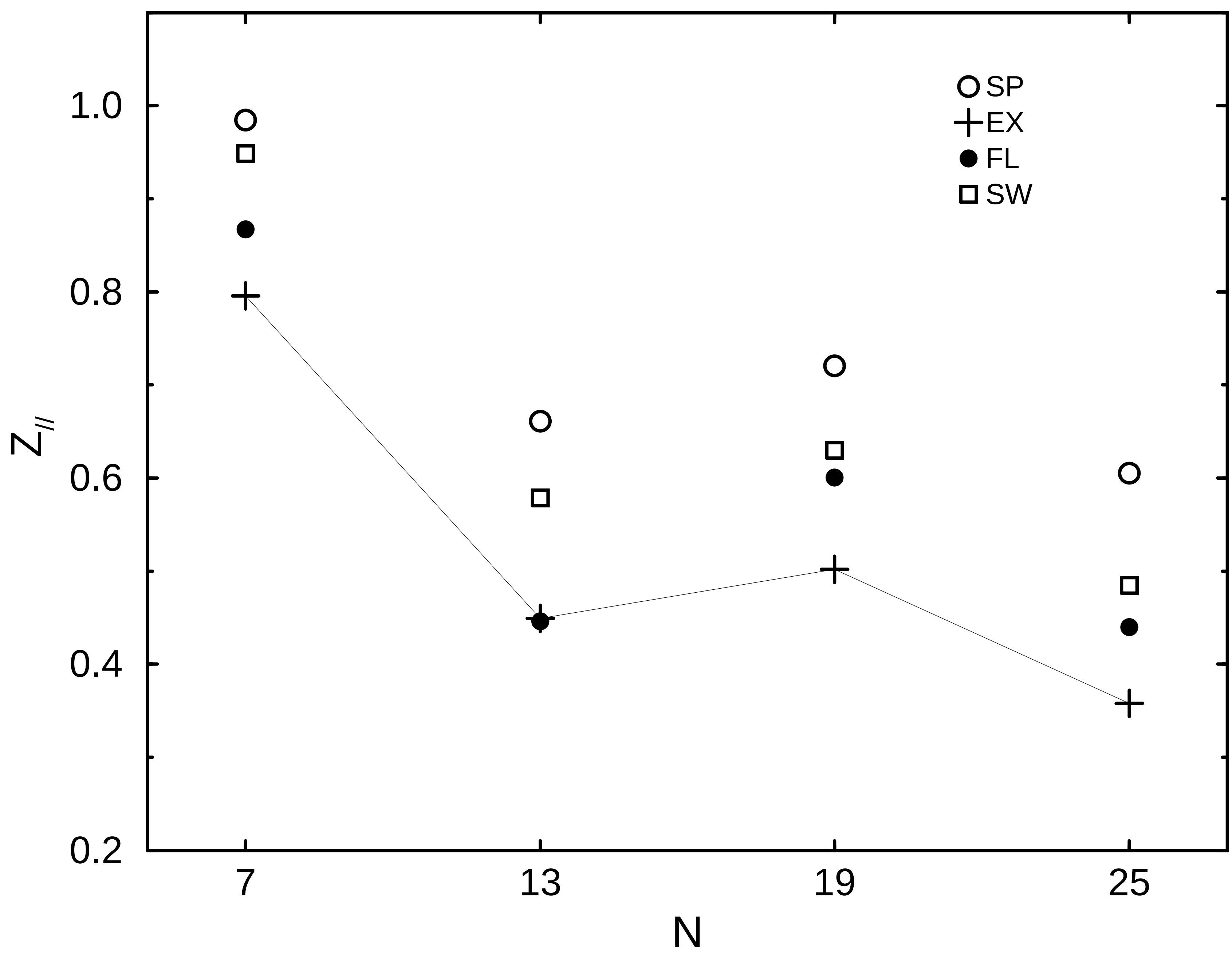

SP
EX
FL
SW
1.0
0.8
0.6
0.4
0.2
$Z_{//}$
7
13
19
25
N

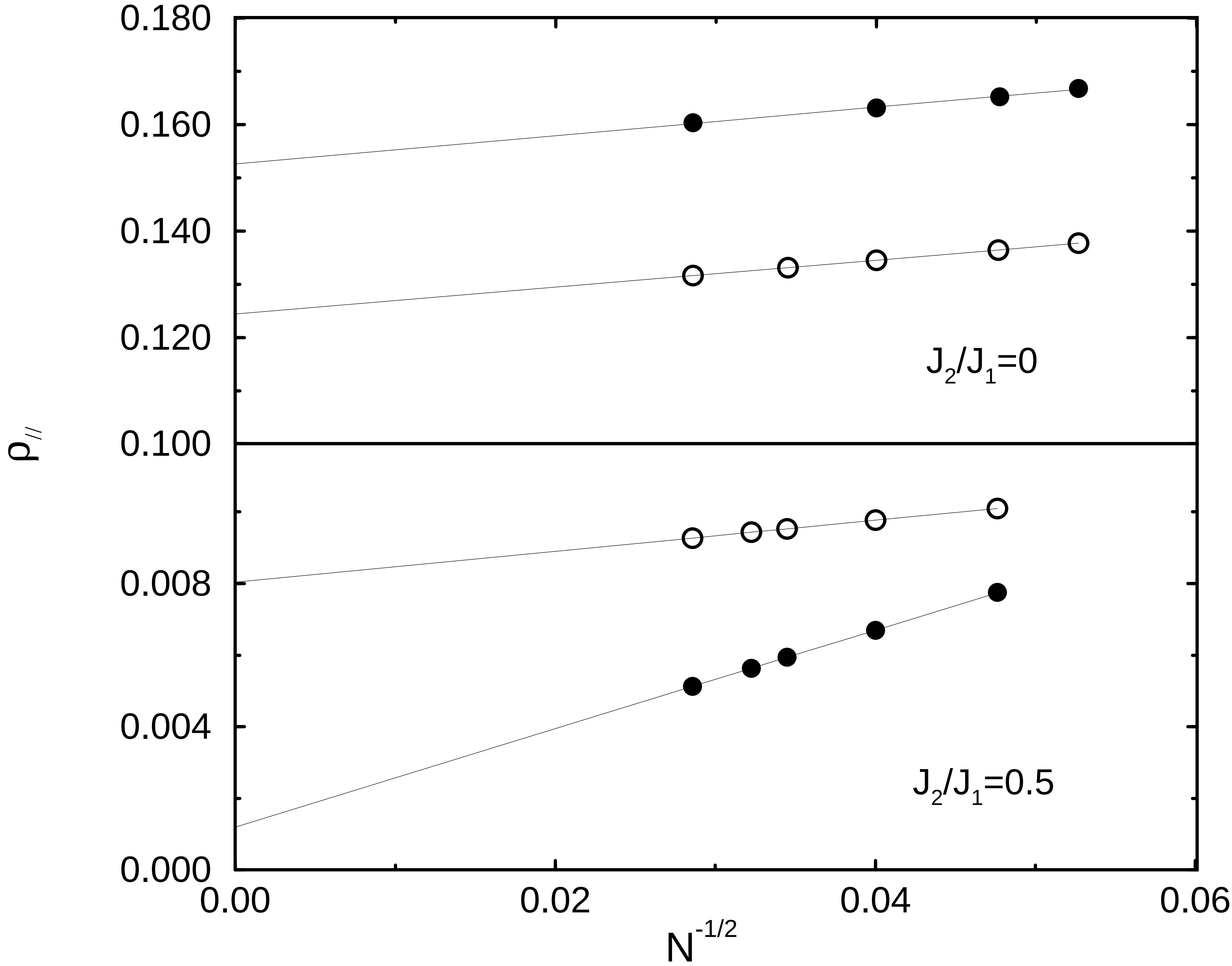

0.180
0.160
0.140
0.120
0.100
0.008
0.004
0.000
0.00
0.02
0.04
0.06
$\rho_{//}$
$N^{-1/2}$
$J_2/J_1=0$
$J_2/J_1=0.5$

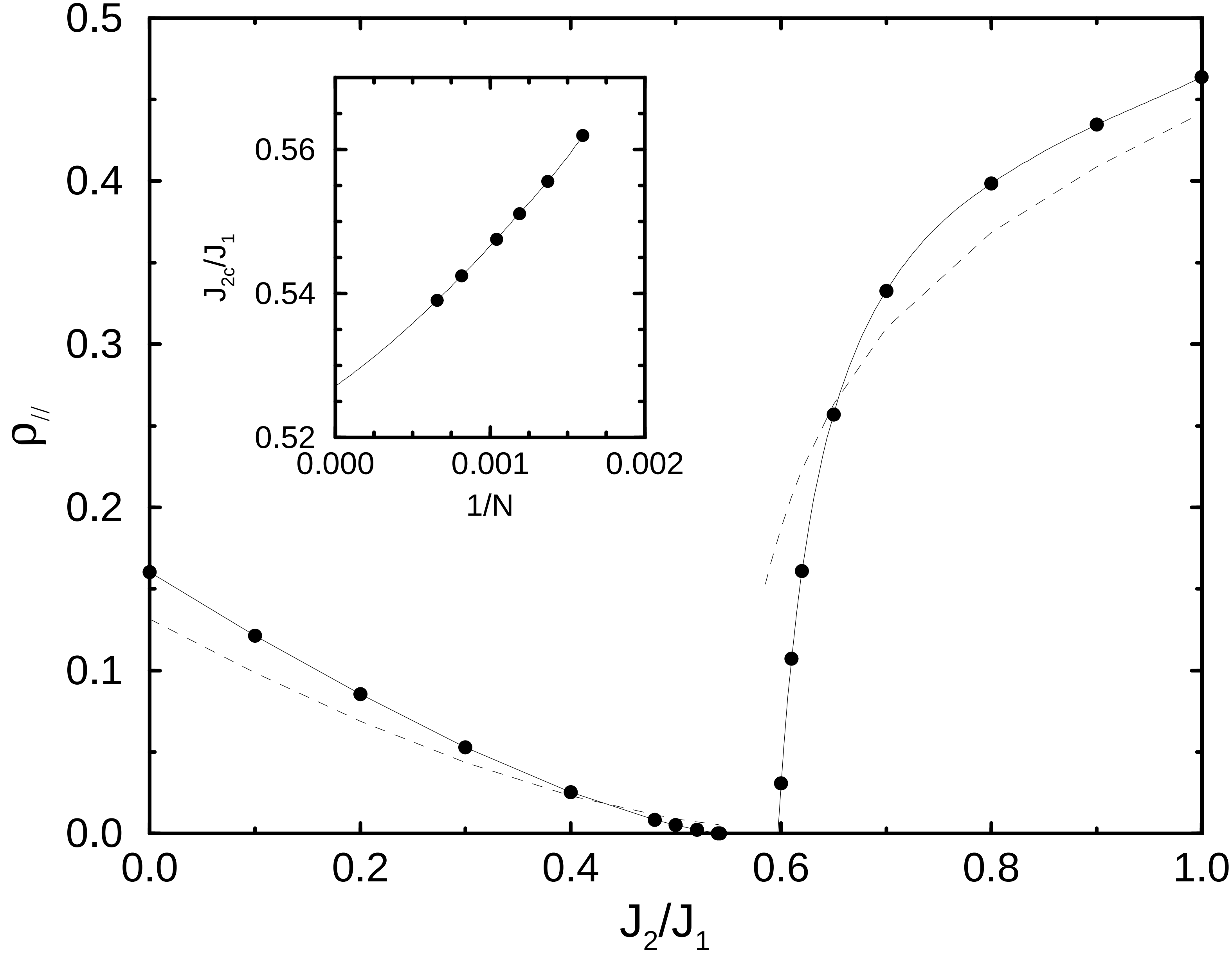

0.5
0.4
0.3
0.2
0.1
0.0
0.0
0.2
0.4
0.6
0.8
1.0
$\rho_{//}$
J_2/J_1
0.56
0.54
0.52
0.000
0.001
0.002
J_{2c}/J_1
1/N

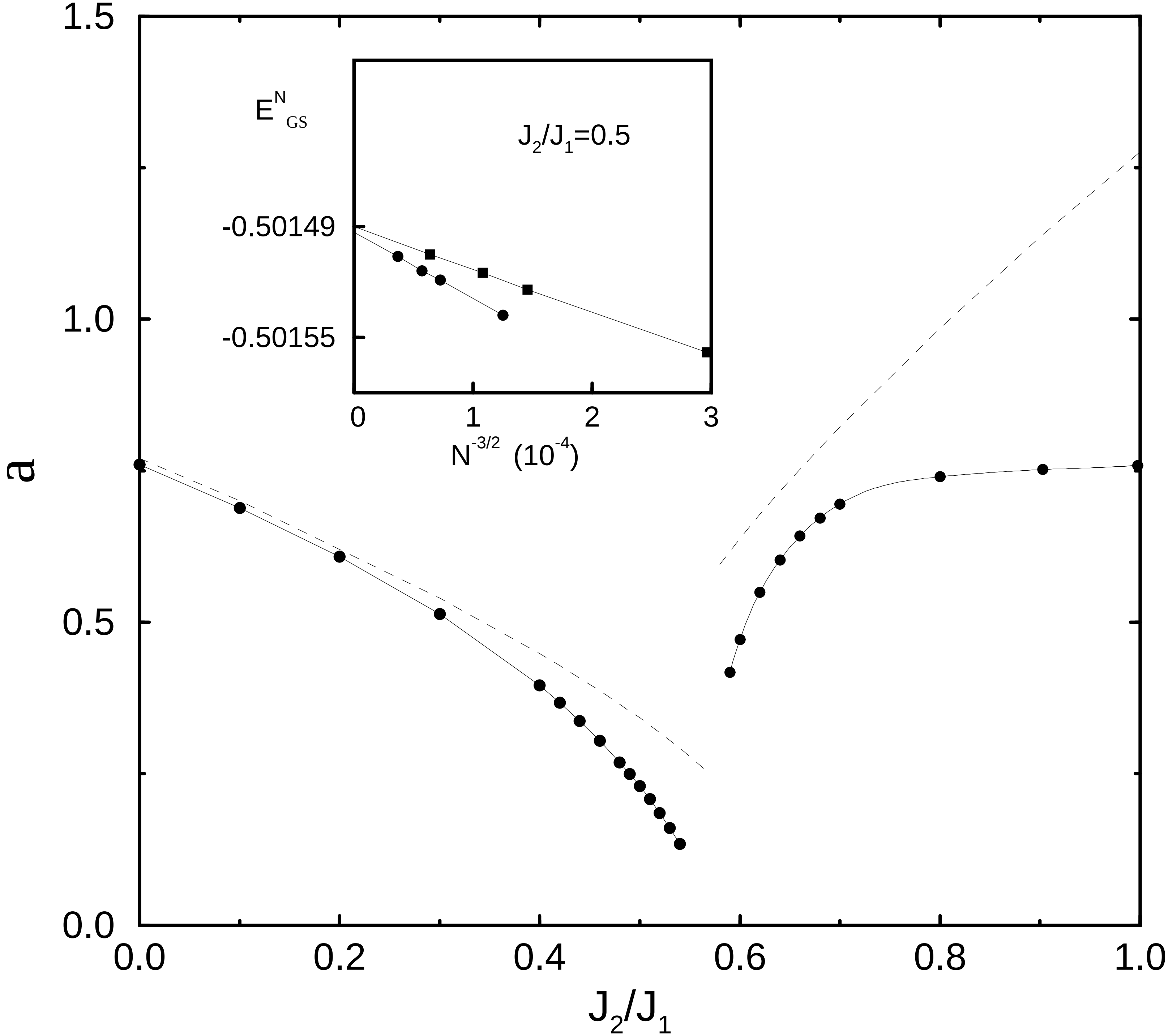

E^N_GS
J_2/J_1=0.5
-0.50149
-0.50155
0
1
2
3
N^-3/2 (10^-4)
1.5
1.0
0.5
0.0
a
0.0
0.2
0.4
0.6
0.8
1.0
J_2/J_1